Structure-properties relationships in triarylamine-based push-pull systems-C60 dyads as active material for single-material organic solar cells

Alexandra Bogdan, Lorant Szolga, Gavril-Ionel Giurgi, Andreea Petronela Crişan, Diana Bogdan, Sarinya Hadsadee, Siriporn Jungsuttiwong, Riccardo Po, Ion Grosu, Jean Roncali

Structure-properties relationships in triarylamine-based push-pull systems-C_{60} dyads as active material for single-material organic solar cells

Alexandra Bogdan,[a] Lorant Szolga,[a,b] Gavril-Ionel Giurgi,[a,b] Andreea Petronela Crişan,[a] Diana Bogdan,[c] Sarinya Hadsadee,[d] Siriporn Jungsuttiwong,[d] Riccardo Po,[e] Ion Grosu*[a] and Jean Roncali*[a,f]

- [a]Babes-Bolyai University, Faculty of Chemistry and Chemical Engineering, Department of Chemistry and SOOMCC, Cluj-Napoca, 11 Arany Janos str., 400028, Cluj-Napoca, Romania
- [b]Optoelectronics Group, Base of Electronics Department, ETTI, Technical University of Cluj-Napoca, Str.Memorandumului, Nr.28, Cluj-Napoca, 400114, Romania
- [c]National Institute for Research and Development of Isotopic and Molecular Technologies, 67-103 Donath str., RO-400293, Cluj-Napoca, Romania
- [d]Center for Organic Electronics and Alternative Energies, Department of Chemistry University of Ubon Ratchathani 34190, Thailand
- [e]Research Center for Renewable Energies and Environment, Instituto Donegani, Eni S. p. A., via Fauser 4, IT-28100 Novara, Italy
- [f]Moltech Anjou CNRS, University of Angers, 2 Bd Lavoisier, 49045, Angers, France

* Corresponding author. E-mail address: jeanroncali@gmail.com (J. Roncali).

Keywords. Single-material, organic solar cells, triarylamine, donor-acceptor

Abstract: The synthesis of a dyad involving a small arylamine-dicyanovinyl push-pull system as donor block and C_{60} fullerene as acceptor, connected by a flexible insulating linker formed by esterification of a β-hydroxymethylthiophene spacer is described. Unlike previously reported parent dyads with linkers connected at the 2-position of the thienyl spacer, this mode of connection allows the preservation of a free carbaldehyde group and thus the possibility to modulate the energy levels of the push-pull donor block. The electronic properties of the new dyad are analyzed by UV-Vis absorption spectroscopy, cyclic voltammetry, and theoretical calculations. A preliminary evaluation of this compound as active material for single-material organic solar cells is reported and discussed with reference to the mode of linkage of donor and C_{60} blocks.

1. Introduction

Organic photovoltaic (OPV) cells have been subject to a continuing research effort for almost forty years [1]. Starting with Shottky diodes delivering short-circuit current densities of a few micro-amps, the performances have been progressively improved, marked by several milestones such as the first vacuum deposited donor-acceptor bilayer planar heterojunction in 1986 [2], the invention of solution-processed polymer-based bulk heterojunction (BHJ) [3], the use of fullerenes as acceptor materials [4], the introduction of soluble molecular donor materials [5] and the recent emergence of non-fullerene molecular acceptors [6,7]. Thanks to these cumulative synergistic research efforts, the *PCE* of BHJ cells is now approaching that of silicon solar cells with values close to 18% [8]. In spite of this impressive progress, the industrialization of OPV cells is still hindered by several problems such as the cost and scalability of active materials [9,10] and the insufficient stability of BHJ cells [11,12]. The fabrication of highly efficient BHJ cells implies the achievement of optimal nano-phase separation of the donor (D) and acceptor (A) materials by optimization of many parameters such as composition of feed solution, solvent, conditions of film processing, additives and application of thermal and/or solvent annealing [13-15]. However, the optimized morphology of multi-component BHJs is thermodynamically unstable and undergoes a progressive phase separation of D and A accompanied by a decrease of *PCE* [11-13].

Single material organic solar cells (SMOSCs) combining D and A parts capable to ensure the elemental processes of light absorption, exciton dissociation and charge-transport can represent a definitive solution to the problem of morphological instability. Furthermore, SMOSCs present major potential advantages in terms of simplicity of fabrication and cost of OPV cells [16,17]. However, the extremely complex fundamental and technical problems posed by the design of active single materials and the widely accepted opinion that fast charge-recombination and inefficient charge transport definitely limits the efficiency of SMOSCs have strongly inhibited research effort in this direction. The design of SMOSC materials resort to two main approaches which basically differ by the degree of intramolecular interaction of the D and A blocks. Fully conjugated molecular D-A systems probably represent the ultimate stage of simplification of SMOSCs and hence of OPV cells but very few examples are known with *PCE*

of 0.40-0.80% [18-20] while the best value reported so far is only of ~1% [21]. Until now, the most widely investigated and most efficient SMOSCs are based on the BHJ model, namely with D and A blocks linked by a flexible insulating spacer allowing the self-organization and nano-scale segregation of the D and A phases. Due to a limited research effort, the highest efficiency of SMOSCs has for a long time stagnated to values of 1.00-1.50 %. However, the past few years have witnessed an acceleration of research and several recent publications reported *PCE* above 3.0 % [22-25] while quite recently, Park *et al* reported a *PCE* of 5.28 % for a cell based on a D-A block copolymer [26], while Weiwei Li and coworkers synthesized double-cable polymers leading to SMOSCs with *PCE* up to 6.30 % [27,28].

In a constant search of scalable active OPV materials combining simple structure and low synthetic complexity we have developed a systematic analysis of structure-properties relationships on simple model systems based on small push-pull molecules involving arylamine donor blocks connected to an electron-withdrawing group by a thienyl spacer [29]. For instance, we have shown that replacing a phenyl group of triphenylamine by a β-naphtyl group (**Nph-A**) (Chart 1) leads to a five-fold increase of hole-mobility and improves the *PCE* of a simple D/A bi-layer planar heterojunction from 2.50 to 3.40 % [30]. In the frame of the extension of this approach to the synthesis of active materials for SMOSCs, we recently reported a dyad with a fullerene C_{60} acceptor unit linked to a donor block derived from **Nph-A** through a cyanoester group (**ECV-C_{60}**) (Chart 1). Evaluated in a simple device (ITO/**ECV-C_{60}**/Al, this compound gives a short-circuit current density (J_{sc}) of 1.90 mA cm^{-2} and a *PCE* of 0.40% [31], while similar results were obtained with other analog dyads [31-33]. In an attempt to improve these results, we report herein the synthesis of a dyad based on **Nph-A** and C_{60} but using a different mode of connection of the D and A blocks. Thus, instead of attaching the C_{60} unit at the 2-position of thiophene through a cyanoester group like in **ECV-C_{60}**, we use the 3-position of the thiophene ring. Although this strategy requires a more complex synthetic approach, it presents two major advantages namely i) the problem of *E/Z* isomerism around the double bond connecting the thienyl ring and the cyanovinyl ester [34] is eliminated and ii) the presence of a free aldehyde group at the 2-position of thiophene during the synthesis (Scheme 1) offers the possibility to modulate the electronic properties of the donor block. This approach is illustrated here with **DCV-C_{60}** in which the cyanoester of **ECV-C_{60}** is replaced by the stronger electron-withdrawing dicyanovinyl group. The synthesis of the new dyad is described and its electronic

properties are analyzed by UV-Vis spectroscopy, cyclic voltammetry and theoretical calculations. The results of a preliminary evaluation of **DCV-C$_{60}$** as active SMOSC material are discussed with reference to **ECV-C$_{60}$** and model compounds of the two donor blocks.

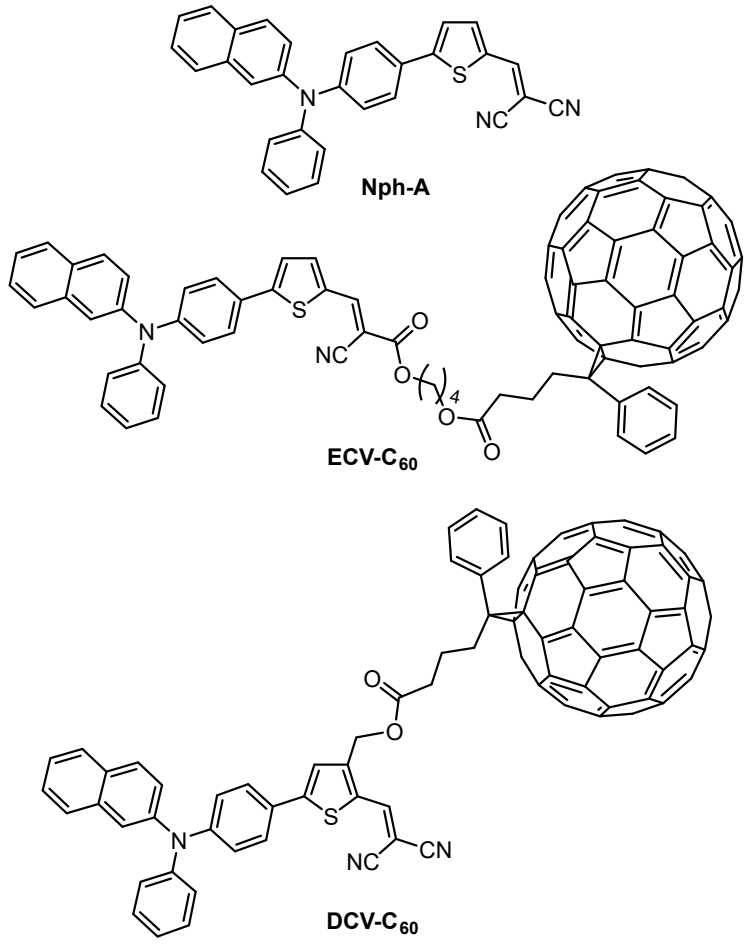

Chart. Chemical structures of **Nph-A**, **ECV-C$_{60}$** and **DCV-C$_{60}$**.

2. Results and discussion

Synthesis

The synthesis of the target compound **DCV-C$_{60}$** is depicted in Scheme 1. Bromination of 3-thienylmethanol **10** with NBS gave the dibromo compound **9** in 62% yield. Reaction of **9** with *tert*-butyldimethylsilylchloride (TBDMSCl)aforded tert-butyl((2,5-dibromothiophen-3-yl)-

methoxy) dimethyl-silane (**8**) in 99% yield. This compound was then reacted with *n*-BuLi and DMF to give the corresponding carbaldehyde **7** in 40 % yield. Suzuki coupling of the commercially available boronic ester **6** with aldehyde **7** gave aldehyde **5** in 62 % yield. This latter compound was then deprotected using tetrabutylammonium fluoride (TBAF) in THF to give the hydroxymethyl aldehyde **4** (yield 88 %). A Knoevenagel condensation of **4** with malonodinitrile in the presence of Et_3N gave the push-pull compound **3** in 87% yield. The final compound **DCV-C$_{60}$** was then synthesized in 48% yield by Steglish esterification, using the already reported procedure [31].

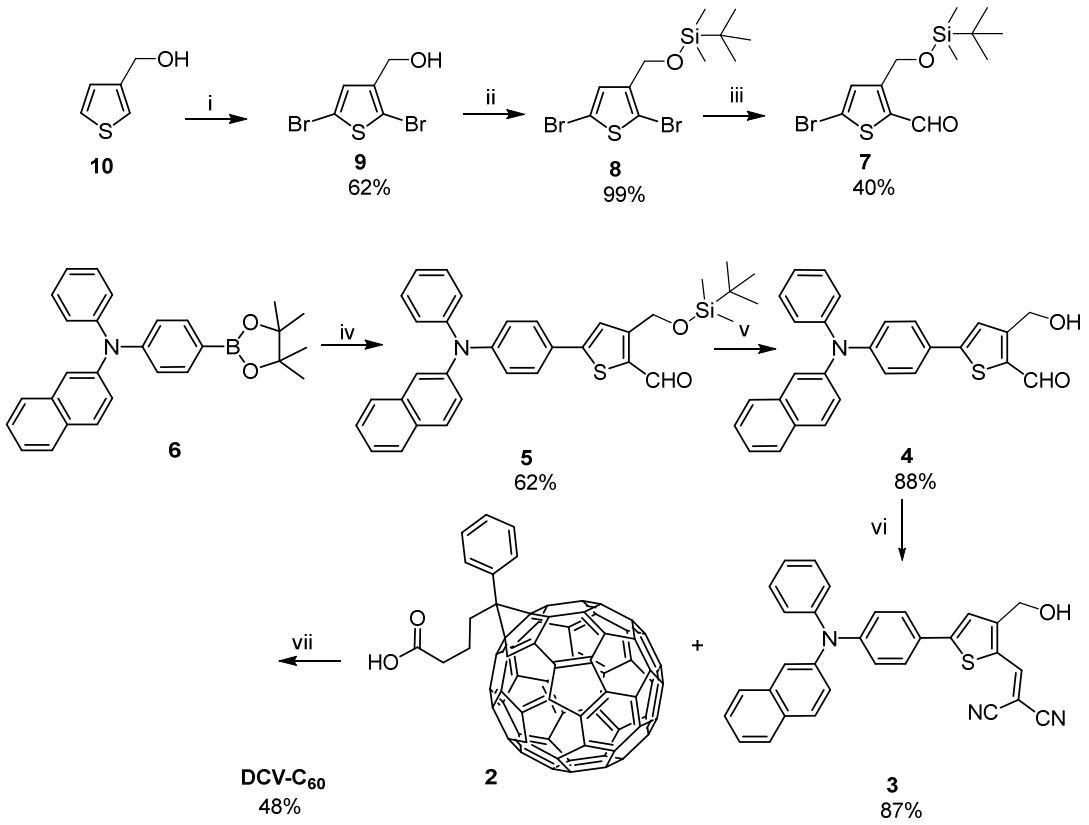

Scheme 1. Synthesis of **DCV-C$_{60}$**: i) NBS, THF; ii) TBDMSCl, *N*-methylimidazole, I_2, THF; iii) n-BuLi, DMF, *n*-Hexane; iv) Cs_2CO_3, $Pd(dppf)Cl_2$, 1,4-dioxane/H_2O; v) TBAF, THF; vi) Malonodinitrile, Et_3N, $CHCl_3$; vii) APTS, DMAP, WSC-HCl, CS_2.

UV-Vis absorption spectroscopy

The optical properties of the hydroxymethyl functionalized donor block **3** and **DCV-C$_{60}$** have been analyzed by UV-Vis spectroscopy of solutions in dichloromethane (DCM) and of thin films spun-cast on glass from DCM solutions. The spectrum of compound **3** exhibits a first band

in the 300–400 nm region attributed to a π–π* transition followed by a more intense band with an absorption maximum (λ_{max}) at 510 nm assigned to an internal charge transfer transition (ICT) [5]. While this spectrum is very similar to that of the parent compound devoid of 3-substituent (compound **2b** in ref 29), the hydroxymethyl linking group produces a 10 nm bathochromic shift of λ_{max} attributed to the electron-withdrawing effect of the oxygen when connected at a β-position of thiophene through a methylene group [35,36]. As shown in Fig. 1, the spectrum of **DCV-C$_{60}$** presents a first transition in the 300-400 nm region due to the combined absorption of the triarylamine block and C_{60}, followed by an ICT band with λ_{max} at 519 nm. Comparison with **ECV-C$_{60}$** shows that the combined electron-withdrawing effects of the methyleneoxy- and dicyanovinyl groups produce a 37 nm bathochromic shift of λ_{max}. Furthermore, compared to the precursor compound **3,** the connection to C_{60} produces a 11 nm red shift of λ_{max} to 519 nm. The absence of intramolecular electronic interaction between the donor block and C_{60} suggests that this phenomenon, already noticed for other dyads [31], could be related to some intermolecular interactions. As generally observed, the absorption spectrum of thin solid films presents a bathochromic shift of λ_{max} from 508 to 538 nm for compound **3** and from 519 nm to 540 nm for **DCV-C$_{60}$** (Fig. 1 and Table 1), due to intermolecular interactions in the solid state, this shift corresponds to a decrease of the optical band gap (E_g) from 2.00 eV for **ECV-C$_{60}$** to 1.90 eV for **DCV-C$_{60}$**.

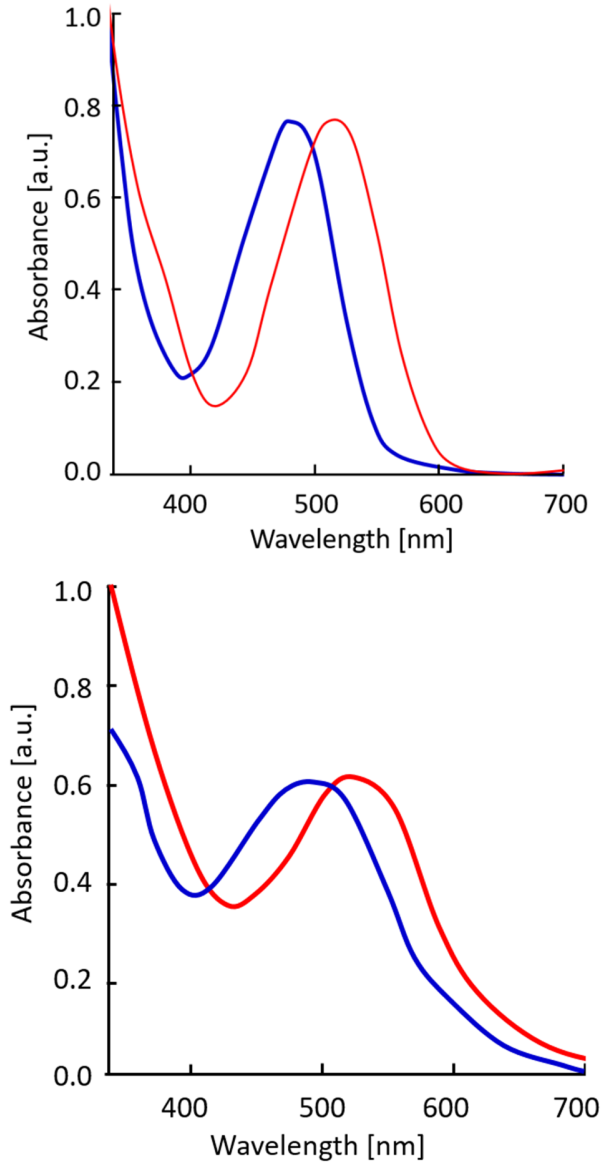

Fig. 1. UV-Vis absorption spectra of **ECV-C_{60}** (Blue) and **DCV-C_{60}** (Red). Top: in DCM., bottom: as thin film spin-cast on glass

Cyclic Voltammetry

The electrochemical properties of **DCV-C_{60}** were investigated by cyclic voltammetry (CV) in DCM in the presence of Bu_4NPF_6 as the supporting electrolyte. The oxidation and reduction processes were analyzed in distinct experiments in order to avoid possible interferences between the process of interest (oxidation or reduction) and the eventual presence of products of degradation of the opposite process.

Table 1.UV-Vis spectroscopy data of 10^{-5} M in DCM; (f): films spin-cast on glass), and results of cyclic voltammetry (in 0.10 M Bu_4NPF_6/DCM, scan rate 100 mV s^{-1}, Pt electrodes, ref. SCE).[a] from Ref 31.[b] from ref 30. Data in bolt correspond to the irreversible reduction of the cyanovinyl ester or dicyanovinyl group. C: estimated from the onset of the oxidation and reduction waves.

Compd	λ_{max}^{s} [nm]	λ_{max}^{f} [nm]	E_g [eV]	logε [$M^{-1}cm^{-1}$]	E_{pa} [V]	E_{pc} [V]	E_{HOMO} [eV][c]	E_{LUMO} [eV][c]
$PC_{61}BM$[a]					-	-0.78, -1.17, -1.67		
Nph-A[b]	500	518	2.00	4.56	1.00	**-1.21**		
3	508	538	1.90	4.47	0.98	**-1.11**		
ECV-C_{60}[a]	482	525	2.00	4.42	0.97	-0.76, -1.14, -**1.29**, -1.65	-5.51	-3.83
DCV-C_{60}	519	540	1.90	4.50	0.97	-0.79, -**1.06**, -1.22, -1.68	-5.53	-4.02

The CV of compound **3** shows a reversible one-electron oxidation wave with an anodic peak potential (E_{pa}) at 0.98 V corresponding to the formation of a stable radical cation of the push-pull-donor block. In the negative potential region, the CV exhibits an irreversible reduction wave with a cathodic peak potential (E_{pc}) at -1.11 V, assigned to the irreversible reduction of the dicyanovinylgroup [30]. Comparison with the CV of **Nph-A** reveals a 100 mV positive shift of E_{pc} due to the electron-withdrawing effect of the hydroxymethyl group at the 3-position of thiophene [35,36]. As shown in Fig. 2, the oxidative CV of **DCV-C_{60}** is practically identical to that of compound **3** with a reversible oxidation wave peaking at 0.97 V. The reduction CV shows reversible cathodic waves with E_{pc} at −0.79, −1.22 and −1.68 V corresponding to successive one-electron reduction processes of the attached C_{60}. Based on the CVs of **3** and **$PC_{61}BM$**, the irreversible cathodic peak at -1.06 V can be assigned to the reduction of the dicyanovinyl group. Comparison with **ECV-C_{60}** shows that this reduction peak is positively shifted by 230 mV due to the stronger electron-withdrawing effect of the dicyanovinyl group.

In order to complete these results, quantum chemical calculations based on density functional methods have been performed with the Gaussian 09 package. Becke's three-parameter gradient corrected functional (B3LYP) with 6-31G(d,p) basis was used to optimize the geometry and to compute the electronic structure.

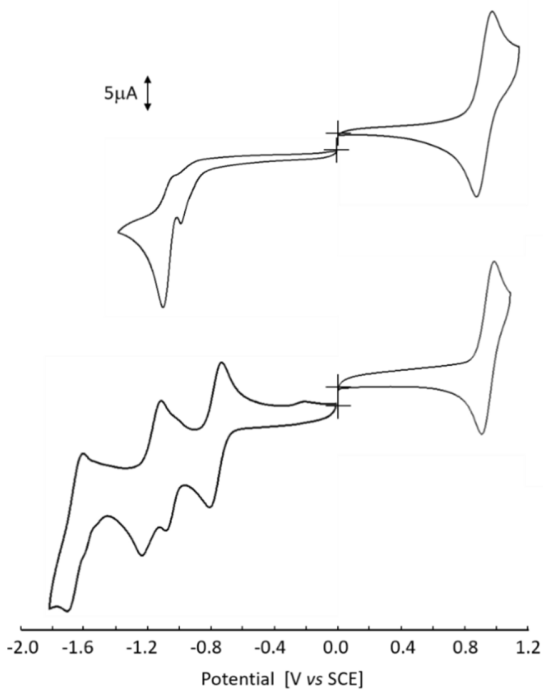

Fig. 2. Cyclic voltammograms corresponding to the oxidation (right) and reduction (left) of compound **3**(top) and **DCV-C_{60}** (bottom) in 0.10 M Bu_4NPF_6/CH_2Cl_2, Pt electrodes, scan rate 100mV s^{-1}.

In order to obtain a more complete description of the energy levels in the dyads, computational work has been extended to compounds **E** and **D** (Chart 2) taken as models of the two types of donor blocks in the corresponding dyads. As expected, the absence of intramolecular electronic interaction between the donor block and C_{60} due to the insulating alkyl spacers, the HOMO of the dyads is localized on the donor block and LUMO on the fullerene units (Fig. 3).

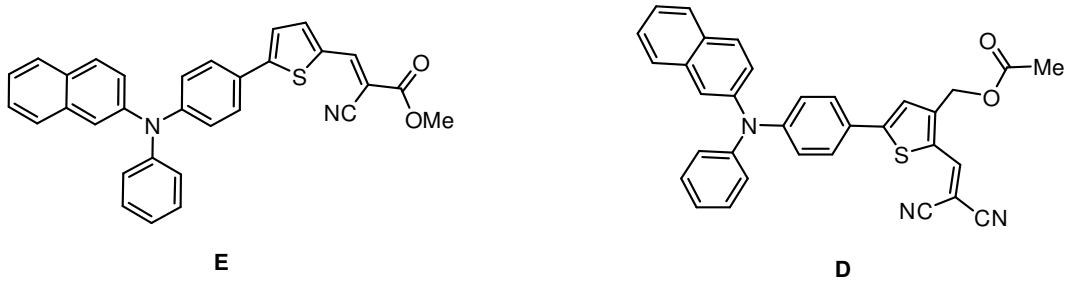

Chart 2. Chemical structure of the model compounds **E** and **D**.

The calculated energy levels of the frontier orbitals are listed in Table 2. The results are in qualitative agreement with the values estimated from the onset of the oxidation and reduction

waves of **ECV-C_{60}** and **DVC-C_{60}**. In agreement with electrochemical data, the calculations suggest that the replacement of the cyanoester by a dicyanovinyl group in the dyad and model compounds leads to a small decrease of the HOMO level but does not affect the LUMO level of the dyads which is determined by the C_{60} unit. However, replacement of the cyano ester by a dicyanovinyl group produces a ~0.30 eV decrease of the LUMO between **E** and **D,** in agreement with the observed 0.23 V positive shift of E_{pc}.

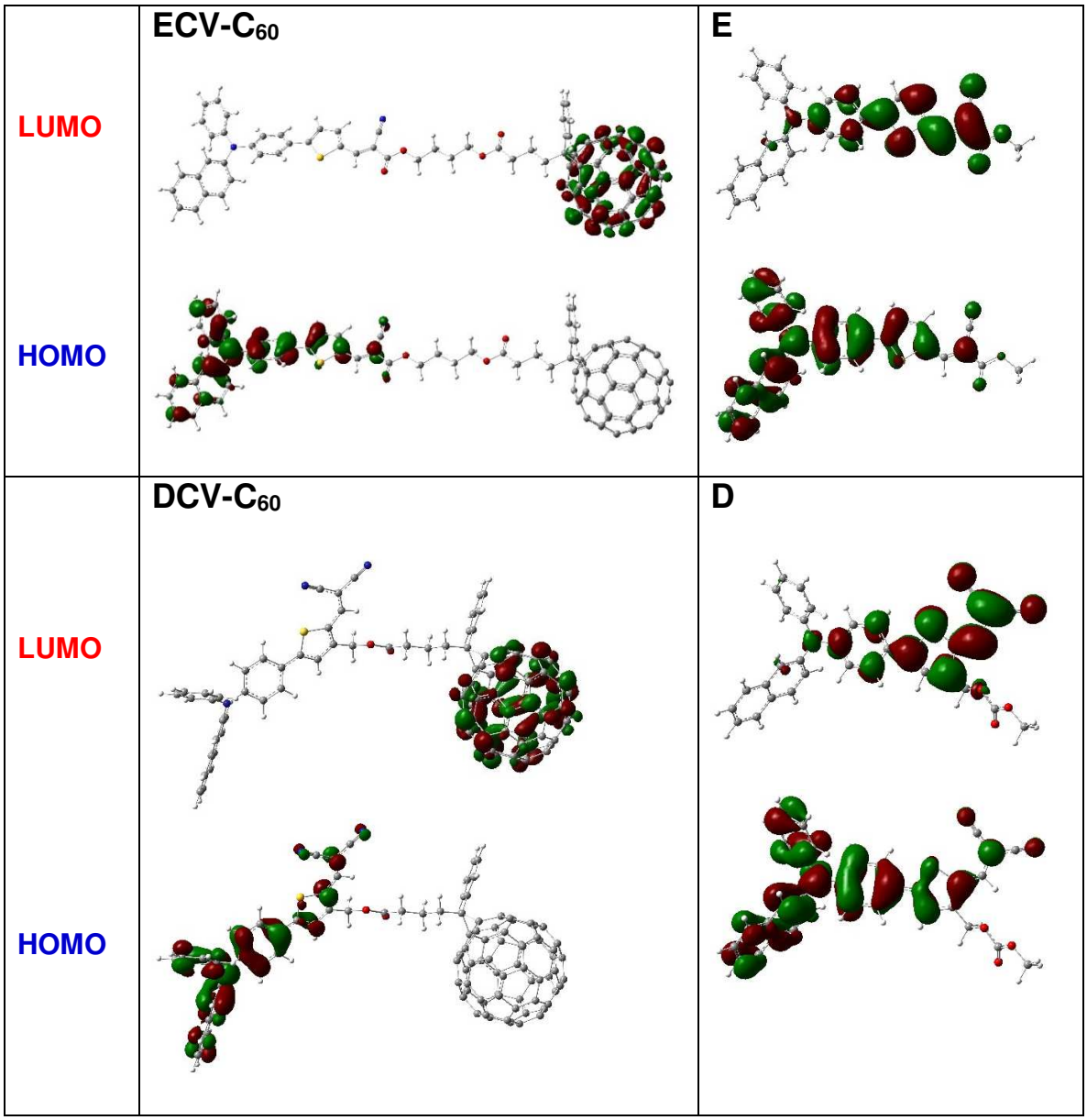

Fig. 3. Distribution of the HOMO and LUMO levels for the dyads and model compounds

However, the calculated decrease of the HOMO level between **ECV-C$_{60}$** and **DCV-C$_{60}$** appears in contradiction with the similar E_{pa} values of these two compounds **Nph-A** and compound **3**. This quasi-insensitivity of the oxidation potential on substitution has been already been observed for many triarylamine-based parent push-pull systems containing a large variety of electron-withdrawing groups [37]. While this problem would certainly deserves further experimental and theoretical investigations, this question is clearly beyond the scope of this work. To summarize, in agreement with optical data that for both dyads and model compounds, these results show that the replacement of the cyanoester by a dicyanovinyl group combined with the oxymethylene substituent at the 3-position produce a *ca* 0.20 eV decrease of the energy gap ΔE of the push-pull donor block which is the main absorbing part of the dyads.(Table 2).

Table 2. Calculated energy levels of the HOMO and LUMO for the dyads and the models molecules and dipole moments of compounds **E** and **D**.

Compd	E_{HOMO} [eV]	E_{LUMO} [eV]	ΔE [eV]	μ [D]
E	-5.18	-2.51	2.67	6.2
ECV-C$_{60}$	-5.21	-3.06	2.15	9.4
D	-5.31	-2.83	2.48	10.3
DCV-C$_{60}$	-5.34	-3.11	2.23	9.4

Photovoltaic properties

The morphology of spin-cast films of **DCV-C$_{60}$** on ITO has been analyzed by atomic force microscopy (AFM). As shown in Fig. 4, the films present a rather discontinuous structure with 1 nm rms consisting of nano-objects of fibrils with no indication of nanoscale phase segregation[14]. This less homogeneous morphology compared to **ECV-C$_{60}$** [31] suggests that **DCV-C$_{60}$** presents limited film-forming properties, presumably because of a lower solubility due to the presence of the dicyanovinyl group and of a shorter alkyl spacer.

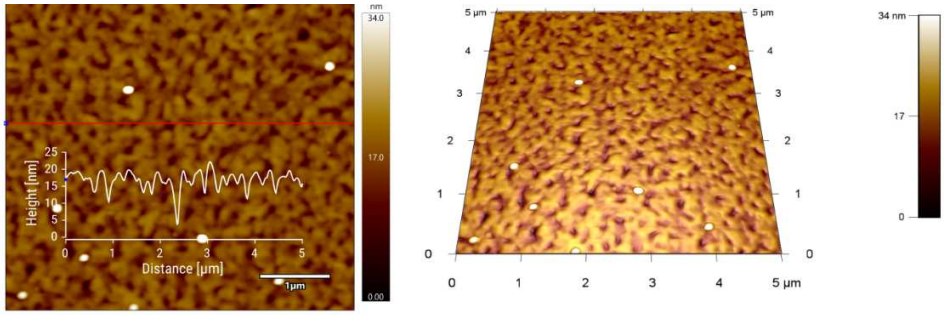

Fig. 4.AFM images and section profile of thin films of **DCV-C60** spun-cast on ITO from a chloroform solution.

A preliminary evaluation of the potential of **DCV-C_{60}** as active material for SMOSC has been performed on inverted cells of structure indium-tin oxide coated glass (ITO)/zinc oxide/active material/molybdene oxide/aluminium. Active layers of ~50 nm thickness were spin-cast in air from chloroform solutions on a 40 nm ZnO layer and the devices were completed by thermal evaporation of a 10 nm film of MoO_3 and 100 nm of aluminium through a shadow mask defining two back electrodes of 28 mm^2 (Fig. 5).

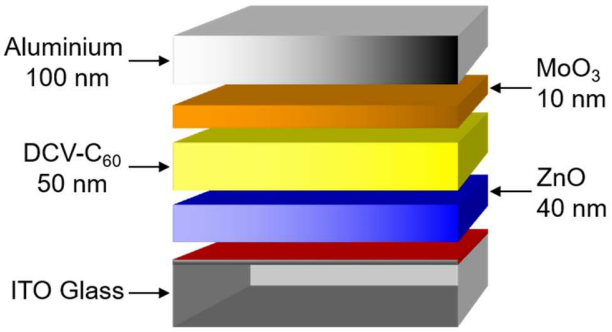

Fig. 5. Structure of the inverted SMOSCs

The current density *vs* voltage curves of SMOSCs based on **ECV-C_{60}** and **DCV-C_{60}** were recorded under AM 1.5 simulated solar illumination with a light power intensity of 100 mW cm^{-2}. Cells based on **ECV-C_{60}** and **DCV-C_{60}** show open-circuit voltage (V_{oc}) and short-circuit current densities (J_{sc}) of 0.70 and 0.96 V and ~3.20 and ~2.80 mA cm^{-2} respectively. Combined with fill factors (*FF*) of ~32 and 29 %, these values lead to *PCE* of ~0.70 and 0.80 % (Table 3). Comparison with previous results on SMOSCs of direct structure based on **ECV-C_{60}** shows that

the inverted cells lead to a noticeable improvement of the photovoltaic characteristics with an increase of J_{sc} from 1.90 to ~3.20 mA cm^{-2} and of *PCE* from ~0.40 to ~0.70 % [31]. The results obtained with **DCV-C$_{60}$** show that in spite of lower J_{sc} and *FF*, *PCE* increases from 0.70 to 0.80 % due essentially to a 0.30 V increase of V_{oc}. Although the *PCE* remains low compared to the best results obtained with donor-acceptor polymers [26-28], it must be underlined that the best two-component cells based on the constitutive blocks of the two dyads gave *PCE* of 3.0-3.5% [29,30].

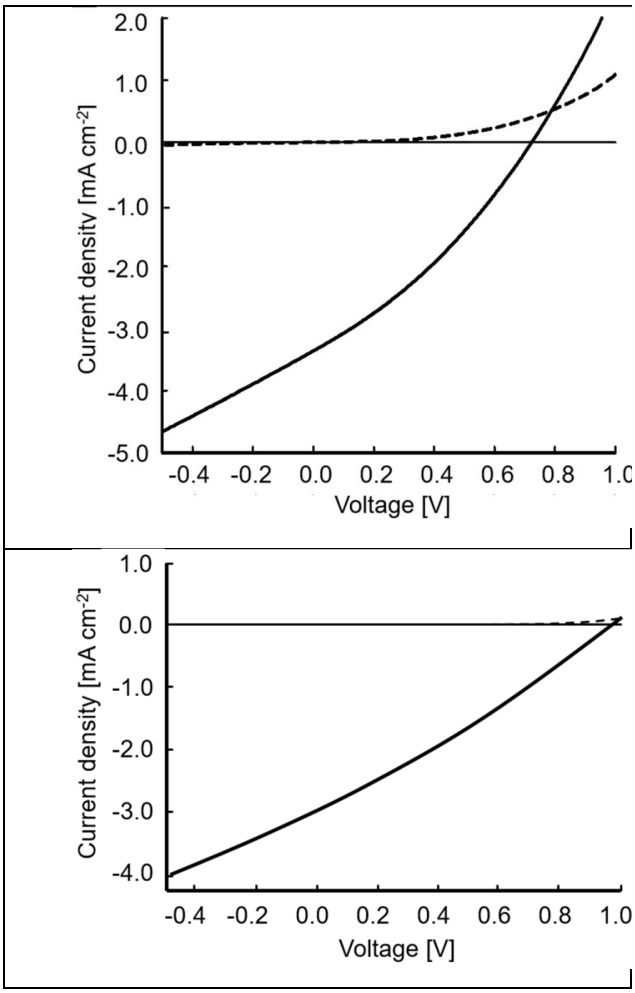

Fig. 6. Current-density *vs* voltage curves for SMOSCs based on **ECV-C$_{60}$** (top) and **DCV-C$_{60}$** (bottom).

It has been shown that the V_{oc} of OPV cells depends on the difference between the energy levels of the HOMO of the donor and LUMO of the acceptor and correlation of V_{oc} with the oxidation potential of the donor or reduction potential of the acceptor have been reported [38,39].

However, more recent work has shown that V_{oc} depends also on other factors such as polarization effects resulting from the modification of the orientation of active molecules [40] or from the desymmetrization of the electronic distribution of donor of A-D-A structure [41]. It has been also shown that the insertion of a monolayer of a strongly dipolar molecule between the donor and the acceptor can produce a significant increase of V_{oc} [42,43]. The data in Table 2 show that whereas **ECV-C$_{60}$** and **DVC-C$_{60}$** show the same dipole moment of 9.4 D, as could be expected from the identical donor and acceptor end blocks, the dipole moment of the push-pull donor block increases from 6.2D for compound **E** to 10.3D for compound **D**. On this basis, it can be proposed that in our SMOSC materials, the strongly dipolar structure of the push-pull donor block plays a role similar to that of a polarized interlayer in bi-component cells. In the frame of this hypothesis, the large increase of V_{oc} observed with **DCV-C$_{60}$** could be related to the larger dipole moment of the push-pull donor block.

Table 3. Photovoltaic characteristics of SMOSCs based on **ECV-C$_{60}$** and **DCV-C$_{60}$.** Average values on six cells, data in bolt are the best results. [a]: Data for direct cell ITO/**ECV-C$_{60}$**/Al from ref. 30

Compd	V_{oc} [V]	J_{sc} [mA cm^{-2}]	*FF* [%]	*PCE* [%]
ECV-C$_{60}$	0.77[a]	1.90[a]	26[a]	0.38[a]
	0.70	3.18	32	0.70
	0.70	**3.33**	**32**	**0.71**
DCV-C$_{60}$	0.96	2.84	29	0.78
	1.00	**2.85**	**28**	**0.80**

Fig. 7 shows the external quantum efficiency responses of the SMOSCs based on the two dyads under monochromatic illumination. The spectra exhibit a first contribution around 400 nm attributed to the contributions of C_{60} and the π–π^* transition of the donor. This first band is followed by a broad band centered at *ca* 500 nm with a maximum of *ca* 20 % corresponding to the ICT of the donor block. As expected from optical data, this main contribution is bathochromically shifted for **DCV-C$_{60}$** due to lower band gap of this material. To summarize these results show that changing the mode of linkage of the D and A blocks offer better possibilities of tuning the optical properties and energy levels of the material and leads to a

noticeable improvement of *PCE* due to a significant increase of the cell voltage. However, the limited processability of the material due to the presence of the dicyanovinyl groups and relatively short alkyl spacer seems to lead to inappropriate morphology and hence poorer charge-transport properties which could explain the lower *FF* and J_{sc} of **DCV-C$_{60}$** compared to **ECV-C$_{60}$**. Consequently, besides the further modulations of the electronic properties offered by the new linking approach further synthetic work will focus on the improvement the processability of the material.

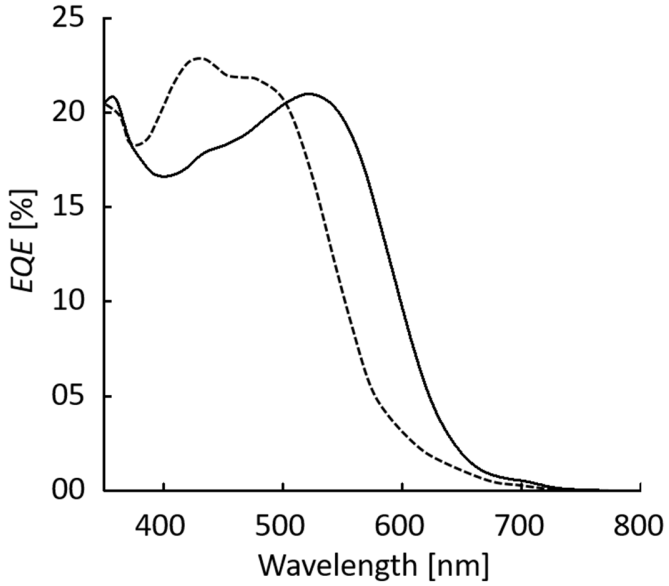

Fig. 7. External quantum efficiency spectra of SMOSCs based on **ECV-C$_{60}$** and **DCV C$_{60}$**

Conclusion

A new molecular dyad consisting of a triarylamine-thienyl-based push-pull π-conjugated system linked to fullerene C_{60} by esterification of an hydroxymethyl group attached at a β-position of the thienyl unit has been synthesized in good yield. Comparison with previously reported SMOSCs based on parent compounds containing similar constitutive blocks shows that this synthetic approach offers further possibilities of tuning of the electronic properties of the donor block and of control of the cell voltage. Thus, these results which contribute to a better understanding of structure-properties relationships in SMOSC materials underline the key role of the mode of linkage of donor and acceptor units in these materials.

Experimental part

All reagents and chemicals from commercial sources were used without further purification. Reactions were carried out under nitrogen atmosphere unless otherwise stated. Solvents were dried and purified using standard techniques. Thin-layer chromatography was performed on Silica gel 60 chromatography plates F_{254}. Column chromatography was performed with analytical-grade solvents using silica gel (tehnical grade, pore size 60 Å). Compounds were detected by UV irradiation or staining with 2,4-dinitrophenylhydrazineor $KMnO_4$ solutions, unless stated otherwise.NMR spectra were recorded with a Bruker AVANCE III 400 or 600 (^1H, 400 or 600 MHz and ^{13}C, 100 or 150 MHz). Chemical shifts are given in ppm relative to TMS and coupling constants *J* in Hz. HR-MS spectra in ESI mode ionization were recorded with an LTQ XL OrbitrapThermoScientific mass spectrometer. UV-Vis measurements were performed in CH_2Cl_2 (HPLC) at room temperature using a Cecil Super Aquarius spectrophotometer. Melting points were measured using a digital KleinfeldApotec melting point apparatus and values are uncorrected. Cyclic voltammetry was performed in DCM solution (HPLC grade). Tetrabutylammoniumhexafluorophosphate (0.10 M as supporting electrolyte) was purchased from Aldrich and was used without purification. Solutions were purged by nitrogen bubbling prior to each experiment. Experiments were carried out in a one-compartment cell equipped with platinum electrodes and saturated calomel reference electrode (SCE) with a Biologic SP-150 potentiostat with positive feedback compensation.

Synthesis

(2,5-dibromothiophen-3-yl)methanol(**9**). *N*-Bromosuccinimide (NBS) (6.5 g, 35 mmol) was added in small portions to a solution of 3-thiophenemethanol (2 g, 17.5mmol) in 150 mL THF at 0 °C. After stirring overnight at room temperature, the reaction mixture was poured into water (50 mL) and extracted with diethyl ether. The organic layer was washed with brine and dried over $MgSO_4$. After removal of the solvent, the crude product was chromatographed on silica gel using petroleum ether/diethyl ether 2:1 as eluent to afford compound **9** (2.95 g) as a transparent oil. Yield: 62 %. ^1H NMR (600 MHz, $CDCl_3$) δ (ppm): 7.02 (s, 1H), 4.56 (s, 2H).

tert-butyl((2,5-dibromothiophen-3-yl)methoxy)dimethylsilane (**8**). To a mixture of **9** (2.5 g, 9.2 mmol) in 100 mL dry THF *N*-methylimidazole (1.65 g, 20.2 mmol), iodine (4.6 g, 18.4 mmol) and *tert*-butyldimethylsilylchloride (1.5 g, 10.1 mmol) were added. The mixture was stirred at room temperature under argon atmosphere for 18 hours. A saturated solution of $Na_2S_2O_3$ was added under stirring and the mixture was extracted with Et_2O. The combined organic layers were washed with water and brine, dried over $MgSO_4$ and evaporated to dryness to give 3.5g of compound **8** as a transparent oil. Yield: 99 %. ^{1}H NMR (400 MHz, $CDCl_3$) δ (ppm): 6.97 (s, 1H), 4.55 (s, 2H), 0.92 (s, 9H), 0.09 (s, 6H).^{13}C NMR (150 MHz, $CDCl_3$) δ (ppm): 142.4, 130.7, 111.0, 107.1, 60.4, 26.0, 18.5, 5.2.

5-bromo-3-(((tert-butyldimethylsilyl)oxy)methyl)thiophene-2-carbaldehyde (**7**)

A solution of **8** (3.4 g, 8.78 mmol) in 150 mL of dry hexane was purged with argon and cooled to -78ºC and *n*-BuLi (3.8 mL, 8.78 mmol, 2.3 M in hexane) was added dropwise. The reaction mixture was stirred for 40 min at -78ºC. DMF (0.82 mL, 10.5mmol) was added at -50°C and the mixture was stirred overnight at room temperature. Water was added and the mixture was extracted with Et_2O. The organic phase was dried over $MgSO_4$ and evaporated to dryness. Column chromatography on silica gel (eluent: pentane/Et_2O 40:1) gave 1.2 g of compound **7** as pale yellow oil. Yield: 40 %. ^{1}H NMR (600 MHz, $CDCl_3$) δ (ppm): 9.97 (s, 1H), 7.16 (s, 1H), 4.97 (s, 2H), 0.93 (s, 9H), 0.12 (s, 6H).); ^{13}C NMR (100 MHz, $CDCl_3$): 181.14, 151.5, 138.6, 132.2, 123.6, 60.2, 25.8, 18.3, -5.4. HRMS: (ESI +), *m/z* calcd for $C_{12}H_{20}BrO_2SSi$ $[M+H]^+$ 335.0131, found 335.0129.

3-(((tert-butyldimethylsilyl)oxy)methyl)-5-(4-(naphthalen-2-yl(phenyl) amino) phenyl) thiophene-2-carbaldehyde (**5**). A mixture of *N*-phenyl-*N*-(4-(4,4,5,5-tetramethyl-1,3,2-dioxaborolan-2-yl)phenyl)naphthalen-2-amine **6** (970 mg, 2.9 mmol), 5-bromo-3-(((tert-butyldimethylsilyl)oxy)methyl)thiophene-2-carbaldehyde **7** (1.2 g, 2.9 mmol) and Cs_2CO_3 (2.8 g, 8.7 mmol) in a mixture of dioxane (80 mL) and water (20 mL) was placed in a round-bottom flask and degassed with argon during 15 min before addition of $Pd(dppf)Cl_2$ (210 mg, 0.29 mmol) as catalyst. The reaction mixture was heated at 100°C for 15 h under an argon atmosphere. After evaporation of the solvent, the residue was dissolved in DCM (100 mL) and the solution was washed with water (2 x70 mL) and brine, dried over $MgSO_4$ and evaporated to dryness. Column chromatography on silica gel (eluent pentane:Et_2O 6:1) gave 1.2 g of **5** as a yellow solid. Yield: 62 %. ^{1}H NMR (600 MHz, $CDCl_3$) δ (ppm): 10.04 (s, 1H), 7.79–7.76 (m,

2H), 7.63 (d, 1H, *J* = 8.4 Hz), 7.52 (d, 2H, *J* = 8.4 Hz), 7.50 (d, 1H, *J* = 2.4 Hz), 7.44–7.38 (overlapped signals, 2H), 7.33–7.29 (overlapped signals, 4H), 7.18 (d, 2H, *J* = 7.2 Hz), 7.13–7.11 (overlapped signals, 3H), 5.04 (s, 2H), 0.94 (s, 9H), 0.13 (s, 6H). ^{13}C NMR (150 MHz, $CDCl_3$) δ (ppm): 182.3, 153.2, 152.5, 149.1, 147.1, 144.7, 134.9, 134.5, 130.7, 129.7, 129.4, 127.8, 127.3, 127.2, 126.7, 126.6, 125.4, 125.2, 124.9, 124.2, 124.0, 122.9, 121.9, 66.0, 60.7, 26.0, -5.1. HRMS: (ESI +), *m/z* calcd for $C_{34}H_{36}NO_2SSi$ $[M+H]^+$ 550.2231, found 550.2239.

3-(hydroxymethyl)-5-(4-(naphthalen-2-yl(phenyl)amino)phenyl)thiophene-2-carbaldehyde **(4)**. Tetrabutylammonium fluoride trihydrate (330 mg, 1 mmol) was added to a solution of derivative **5** (160 mg, 0.37 mmol) in 10 mL THF. The reaction mixture was stirred at room temperature for 30 minutes. The solvent was evaporated and the residue was purified by column chromatography on silica gel using diethyl ether as eluent. Yield: 110 mg (88 %) .^{1}H NMRδ_H(600 MHz, $CDCl_3$) ppm: 9.97 (s, 1H), 7.80–7.77 (overlapped signals, 2H), 7.63 (d, *J* = 7.8 Hz, 1H), 7.53–7.51 (overlapped signals, 3H), 7.44–7.39 (overlapped signals, 2H), 7.33–7.29 (overlapped signals, 4H), 7.19 (d, *J* = 7.8 Hz, 2H), 7.18 (d, *J* = 7.8 Hz, 1H), 7.11 (d, *J* = 8.4 Hz, 2H), 4.89 (d, *J* = 3.6 Hz, 2H).). ^{13}C NMR (100 MHz, $CDCl_3$): 182.7, 154.4, 151.5, 149.4, 147.0, 144.6, 135.4, 134.5, 130.7, 129.7, 129.4, 127.8, 127.3, 127.2, 126.6, 125.5, 125.2, 124.9, 124.3, 122.7, 122.0, 66.0, 59.8. HRMS: (ESI +), *m/z* calcd for $C_{28}H_{22}NO_2S$ $[M+H]^+$ 436.1365, found 436.1364.

2-((3-(hydroxymethyl)-5-(4-(naphthalen-2-yl(phenyl)amino)phenyl)thiophen-2-yl) methylene) malononitrile (**3**).Two drops of Et_3N were added to a mixture of compound **4**(250 mg, 0.574mmol) and malononitrile (115 mg, 1.72 mmol) in $CHCl_3$ (40 mL). The reaction mixture was refluxed for 5 h. After solvent evaporation, chromatography on silica gel with 4:1 Et_2O/pentane as eluent gave 240 mg of a deep red solid. Yield: 87 %. ^{1}H NMR δ_H (600 MHz, $CDCl_3$) ppm: 8.11 (s, 1H), 7.81–7.78 (overlapped signals, 2H), 7.64 (d, *J* = 7.8 Hz, 1H), 7.54 (d, *J* = 9 Hz, 2H), , 7.53 (d, *J* = 1.8 Hz, 1H), 7.45–7.41 (overlapped signals, 2H), 7.35–7.29 (overlapped signals, 4H), 7.19 (d, *J* = 7.8 Hz, 2H), 7.15 (m, 1H), 7.09 (d, *J* = 9 Hz, 2H), 4.86 (s, 2H). ^{13}C NMRδ_C(150MHz, $CDCl_3$)ppm: 155.6, 153.5, 150.1, 148.2, 146.7, 144.3, 134.5, 130.9, 129.8, 129.6, 129.4, 127.9, 127.8, 127.3, 126.7, 125.8, 125.4, 125.1, 125.0, 124.7, 124.0, 122.5, 122.1, 115.1, 114.1, 74.5, 59.2. . HRMS: (ESI +), *m/z* calcd for $C_{31}H_{22}N_3OS$ $[M+H]^+$ 484.1478, found 484.1472.

Target compound (**DCV-C_{60}**): To a degassed solution of the fullerene derivative **2**, (45 mg, 0.05 mmol), 14 mg of *p*-toluene sulfonic acid (*p*-TsOH, 0.075 mmol), 9 mg of 4-dimethylaminopyridine(DMAP, 0.075 mmol) and 14 mg of 1-(3-dimethylaminopropyl)-2-ethylcarbodiimidehydrochloride (WSC–HCl, 0.075 mmol) in CS_2, compound **3** (36 mg, 0.075 mmol) was added. The mixture was stirred after night at room temperature. After removal of the solvent under reduced pressure, the residue was chromatographed on silica gel using DCM to give 33 mg of the the target compound. black purple solid. Yield: 48 %. Mp: 210-212°C. R_f = 0.54 (silicagel, CH_2Cl_2).^{1}H NMR (600 MHz, $CDCl_3$)δ ppm: 7.97 (s, 1H), 7.91 (d, 2H, J = 8.8 Hz), 7.82-7.77 (overlapped signals, 2H), 7.63 (d, 1H, J = 7.5 Hz), 7.54-7.51 (overlapped signals, 5H), 7.48-7.41 (overlapped signals, 3H), 7.35-7.31 (overlapped signals, 3H), 7.29 (dd, 1H, J = 8.8, 2.2 Hz), 7.18 (d, 2H, J = 7.5 Hz), 7.15 (t, 1H, J = 7.4 Hz), 7.07 (d, 2H, J = 8.8 Hz), 5.21 (s, 2H), 2.91-2.85 (m, 2H), 2.60 (t, 2H, J = 7.3 Hz), 2.23-2.16 (m, 2H). ^{13}C NMR (100 MHz, $CDCl_3$): 172.57, 164.95, 150.19, 148.80, 148.03, 147.78, 147.41, 145.89, 145.34, 145.28, 145.19, 144.95, 144.79, 144.66, 144.54, 144.17, 143.91, 143.15, 143.03, 142.26, 141.13, 138.07, 137.71, 136.73, 136.25, 134.44, 132.21, 130.93, 129.84, 129.60, 128.65, 128.49, 127.85, 127.73, 127.35, 126.81, 126.75, 126.52, 125.82, 125.50, 125.01, 124.36, 123.69, 122.59, 122.30, 122.01, 121.46, 119.98, 113.79, 87.52, 62.55, 58.61, 52.59, 51.70, 34.37, 33.88, 33.56, 32.64, 29.85, 27.87, 22.39, 15.43, 11.56. HRMS: (ESI+): *m/z* calcd. for $C_{102}H_{31}N_3O_2S$ [M] + 1362.2165, found 1362.2218.

Device fabrication and characterization

The morphology of the films was analyzed in ambient atmosphere by atomic force microscopy (AFM) using a Cypher S (Asylum Research, Santa Barbara, California, SUA) equipment. Image processing was performed with the dedicated software: Asylum AR v16 and IgorPro (6.38B01). The photovoltaic performances of the two dyads were evaluated on 28 mm^2 active area SMOSCs of inverted structure: ITO/ZnO/dyad/MoO_3/Al. Indium-tin oxide coated glass slides of 24×25×1.1 mm with a sheet resistance of R_S = 7 Ω/sq were purchased from Praezisions Glas & Optik GmbH. The ITO layer was patterned by a 37% hydrochloric acid solution and zinc powder etching. The substrates were then washed with a diluted Deconex® 12 PA-x solution (2% in water) and scrubbed using dish washing soap before being cleaned by a

series of ultrasonic treatments for 15 min in distilled water (15.3 MΩ cm^{-1}), acetone and isopropanol. Once dried under a steam of nitrogen, a UV-ozone plasma treatment (UV/Ozone ProCleaner Plus, Bioforce Nanosciences) was performed for 15 min. The ZnO Layer (40 nm) was deposited from a solution of 198 mg of zinc acetate and 0.54 mL of ethanolamine in 6 mL of ethanol. The solution was stirred at 100°C for 12h, spun-cast on ITO substrates and thermally annealed at 200°C for 1h. The active layer was then spun-cast in ambient atmosphere from a 15 mg/mL chloroform solution and the devices were completed by successive thermal evaporation of MoO_3 (10 nm) and aluminium (100 nm) at a pressure of 1.5×10^{-6} Torr through a shadow mask defining two cells of 28 mm^2 on each ITO substrate. *Jvs V* curves were recorded in the dark and under illumination using a Keithley 236 source-measure unit and a home-made acquisition program. The light source is an AM1.5 Solar Constant 575 PV simulator (Steuernagel Lichttecknik, equipped with a metal halogen lamp). The light intensity was measured by a broad-band power meter (13PEM001, Melles Griot). *EQE* was measured under ambient atmosphere using a halogen lamp (Osram) with an Action Spectra Pro 150 monochromator, a lock-in amplifier (Perkin-Elmer 7225) and a S2281 photodiode (Hamamatsu).

References

[1] Chamberlain G A. Organic solar cells. Solar Cells 1983; 8: 47.

[2] Tang C W. Two-layer organic photovoltaic cell. Appl Phys Lett 1986; 48: 183.

[3] Halls J J M, Walsh C A, Greenham N C, Marseglia E A, Friend R H, Moratti S C, Holmes A B. Efficient photodiodes from interpenetrating polymer networks. Nature 1995; 376: 498.

[4] Yu G, Gao J, Hummelen J C, Wudl F , Heeger A J. Polymer Photovoltaic Cells: Enhanced Efficiencies via a Network of Internal Donor-Acceptor Heterojunctions. Science 1995; 270: 1789.

[5] Roquet S, Cravino A, Leriche P, Alévêque O, Frère P, Roncali J. Triphenylamine-thienylenevinylenes Hybrid Systems with Internal Charge-transfer as Donor Materials for Hetero-junction Solar Cells. J Am Chem Soc 2006; 128: 3459.

[6] Eftaiha A F, Sun J-P, Hill I G, Welch G C. Recent advances of non-fullerene, small molecular acceptors for solution processed bulk heterojunction solar cell. J Mater Chem A 2014; 2: 1201.

[7] Zhang G, Zhao J, Chow P C Y, Jiang K, Zhang J,Zhu Z,Zhang J, Huang F, Yan H. Non fullerene acceptors molecules for bulk heterojunction organic solar cells. Chem Rev 2018; 118: 3447.

[8] Zhang J, Xian K, Zhang T, Hong L, Wang Y, Xu Y, Ma K, An C, He C, Wie Z, Gao F, Hou J. Cui Y, Yao H. Single-Junction Organic Photovoltaic Cells with Approaching 18% Efficiency. Adv Mater 2020; 32: 1908205.

[9] Po R, Bianchi G, Carbonera C, Pellegrino. "All That Glisters Is Not Gold": An Analysis of the Synthetic Complexity of Efficient Polymer Donors for Polymer Solar Cells. Macromolecules 2015; 48: 453.

[10] Po R, Roncali J. Beyond efficiency: scalability of molecular donors for organic photovoltaics. J Mater Chem C 2016; 4: 477.

[11] Gholamkhass B, Holdcroft S. Toward stabilization of domains in polymer bulk heterojunction films. Chem Mater 2010; 22: 5371.

[12] Cheng P, Zhan X. Stability of organic solar cells: challenges and strategies. Chem Soc Rev 2016; 45: 2544.

[13] Brabec C J., Gowrisanker S, Halls J J M, Laird D, Jia S, Williams S P. Polymer-fullerene bulk heterojunction solar cells. Adv Mater 2010; 22: 3839.

[14] Huang Y, Kramer, A. J. Heeger A J, Bazan G C. Bulk Heterojunction solar cells: morphology and performances. Chem Rev 2014; 114: 7006.

[15] McDowell C, Abdelsamie M, Toney M F, Bazan G C. Solvent Additives: Key Morphology-Directing Agents for Solution-Processed Organic Solar Cells. Adv Mater 2018; 30: 1707114.

[16] Roncali J. Single-material organic solar cells: the next frontier for organic photovoltaics. Adv Energy Mater 2011; 1: 147.

[17] Roncali J, Grosu I. The dawn of single-material organic solar cells. Adv Sci 2019; 6: 1801026.

[18] Cravino A, Leriche P, Alévêque O, Roquet S, Frère P, Roncali J. Light-Emitting Organic Solar Cells Based on a 3D Conjugated System with Internal Charge Transfer. Adv Mater 2006; 18: 303.

[19] Di Maria F, Biasiucci M, Paolo Di Nicola F, Fabiano E, Zanelli A, Gazzano M, Salatelli E, Lanzi M, Della Sala F, Gigli G, Barbarella G. Nanoscale Characterization and Unexpected Photovoltaic Behavior of Low Band Gap Sulfur-Overrich-Thiophene/Benzothiadiazole Decamers and Polymers. J Phys Chem C 2015; 119: 27200.

[20] Marinelli M, Lanzi M, Liscio A, Zanelli A, Zangoli M, Di Maria F, Salatelli E. Single-material organic solar cells with fully conjugated electron-donor alkoxy-substituted bithiophene units and electron-acceptor benzothiadiazole moieties alternating in the main chain. J Mater Chem C 2020; 8: 4124.

[21] Balakirev D O, Luponosov Y N, Mannanov A L, Savchenko P S,Minenkov Y, Paraschuk D Y, Ponomarenko S A. Star-shaped benzotriindole-based donor-acceptor molecules: synthesis, properties and application in bulk heterojunction and single-material organic solar cells. Dyes and Pigments 2020; 181: 108523.

[22] Lee J H, Kim A, Kim H J, Kim Y, Park S, Cho M J, Choi D H. High Performance Polymer Solar Cell with Single Active Material of Fully Conjugated Block Copolymer Composed of Wide-Bandgap Donor and Narrow-Bandgap Acceptor Blocks. ACS Appl. Mater. Interfaces 2018; 10: 18974.

[23] Lucas S, Leydecker T, Samori P, Mena-Osteriz E, Bauerle P. Covalently linked donor-acceptor dyad for efficient single material organic solar cells. Chem Commun 2019; 55: 14202.

[24] Li C, Wu X, Sui X, Wu H, Wang C, Feng G, Wu Y, Liu F, Liu X, Tang Z. Li W. Crystalline Cooperativity of Donor and Acceptor Segments in Double-Cable Conjugated Polymers toward Efficient Single-Component Organic Solar Cells. Angew Chem Int Ed 2019; 58: 15532.

[25] Wang W, Sun R, Guo J, Guo J, Min J. An Oligothiophene–Fullerene Molecule with a Balanced Donor–Acceptor Backbone for High-Performance Single-Component Organic Solar Cells. Angew Chem Int Ed 2019; 58: 14556.

[26] Park C G, Park, S H, Kim Y, Nguyen T L, Woo H Y, Kang H, Yoon H J, Park S, Cho M J, Choi D H. Facile one-pot polymerization of a fully conjugated donor–acceptor block copolymer and its application in efficient single component polymer solar cells. J Mater Chem A 2019; 7: 21280.

[27] Feng G, Li J, He Y, Zheng W, Wang C, Li V, Tang Z, Osvet A, Li N, Brabec C J, Yi Y, Yan H, Li W. Thermal-Driven Phase Separation of Double-Cable Polymers Enables Efficient Single-Component Organic Solar Cell. *Joule*, 2019; 3: 1765.

[28] Yu P, Feng G, Li J, Li C, Xu Y, Xiao C, Li W. A Selenophene Substituted Double-cable Conjugated Polymer Enables Efficient Single-Component Organic Solar Cells. J. Mater. Chem.C 2020; 8: 2790.

[29] Roncali J, Leriche P, Blanchard P. Molecular materials for organic photovoltaics: Small is beautiful. Adv Mater 2014; 14: 2821.

[30] Mohamed S, Demeter D, Laffitte J-A, Blanchard P ; Roncali J. Structure-properties relationships in triarylamine-based donor-acceptor molecules containing naphtyl groups as donor material for organic solar cells. Sci Rep 2015; 5: 9031.

[31] Diac A, Szolga L, Cabanetos C, Bogdan A, Terec A, Grosu I, Roncali J. C_{60}-small arylamine push-pull dyads for single-material organic solar cells. Dyes & Pigments 2019; 171: 107748.

[32] Labrunie A, Gorenflot J, Babics M, Aleveque O, Dabos-Seignon S, Balawi A H, Kan Z, Wohlfahrt M, Levillain E, Hudhomme P, Beaujuge P M, Laquai F, Cabanetos C, Blanchard P. Triphenylamine-based push–pull σ–C_{60} dyad as photoactive molecular material for single-component organic solar cells: synthesis, characterizations, and photophysical properties. Chem Mater 2018; 30: 3474.

[33] Labrunie A, Lebailly T, Habibi A H, Dalinot C, Jiang Y, Dabos-Seignon S, Roncali J, Blanchard P, Cabanetos C. CuAAC-Based Assembly and Characterization of a New Molecular Dyad for Single Material Organic Solar Cell. Metals 2019; 9: 618.

[34] Liu Y, Wan X, Wang F, Zhou J, Long G, Tian J, Chen Y. High-performance solar cells using a solution-processed small molecule containing benzodithiophene unit. Adv Mater 2011; 23: 5387.

[35] Roncali J, Garreau R, Delabouglise D, Garnier F, Lemaire M. A molecular approach of polythiophene functionalization. Synth Met 1989; 28: C341-C348.

[36] Lemaire M, Garreau R, Roncali J, Delabouglise D, Korri H, Garnier F. Design of Poly(thiophenes) Containing Oxyalkyl Substituents. New J Chem 1989; 13: 863.

[37] Jeux V, Segut O, Demeter D, Alévêque O, Leriche P, Roncali J. Push–Pull Triphenylamine Chromophore Syntheses and Optoelectronic Characterizations. ChemPlusChem 2015; 4: 697.

[38] Brabec C J, Cravino C, Meissner D, Sariciftci N S, Fromherz T, Rispens M T, Sanchez L, Hummelen J.C. Origin of the open-circuit voltage of organic solar cells. Adv Funct Mater 2001; 11: 374.

[39] Gadisa A, Svensson M, Andersson M R, Inganäs O. Correlation between oxidation potential and open-circuit voltage of composite solar cells based on blends of polythiophenes and fullerene derivative. Appl Phys Lett; 2004; 84: 1609.

[40] Duhm S, Heimel G, Salzmann I, Glowatzki H, Johnson RL, Vollmer A, Rabe JP, Koch, N, Orientation-dependent ionization energies and interface dipoles in ordered molecular assemblies. Nature Mater 2008 ; **7** : 326.

[41] Demeter D , Rousseau T, Leriche P, Cauchy T, Po R, Roncali J, Manipulation of the Open-Circuit Voltage of Organic Solar Cells by Desymmetrization of the Structure of Acceptor-Donor-Acceptor Molecules. Adv Funct Mater 2011; 21:4379.

[42] Qi B, Wang J. Open-circuit voltage in organic solar cells. J. Mater Chem 2012; 22: 24315.

[43] Tada A, Geng Y, Wei Q, Hashimoto K, Tajima K, Nat Mater 2011; 10: 450.

Acknowledgments

This work was financially supported by the project SMOSCs, ID: 37_220, Cod MySMIS:103509 funded by the Romanian Ministry for European Funds through the National Authority for Scientific Research and Innovation (ANCSI) and co-funded by the European Regional Development Fund/Competitiveness Operational Programme 2014-2020 (POC) Priority Axis 1/Action 1.1.4.

Highlights

- A new donor-acceptor dyad based on a small push-pull donor block and C_{60} as active material for single material organic solar cells.
- Analysis of the effect of the mode connection of the donor and acceptor blocks
- Connection through the 3-position of thiophene instead of 2-position allows the modulation of the electronic properties of the donor block
- Single material organic solar cells of inverted structure with improved voltage and efficiency